ATOMICS INTERNATIONAL
A Division of North American Aviation, Inc.

MASTER

NAA-SR-MEMO-3552

This document contains 30 pages

This is copy ___ of ___ series ___

Do not remove this sheet

UNCLASSIFIED

Security Classification

NAA-SR-MEMOs are working papers and may be expanded, modified, or withdrawn at any time, and are intended for internal use only.

This report may not be published without the approval of the Patent Branch, AEC. Released 8/1/61

DISCLAIMER

This report was prepared as an account of work sponsored by an agency of the United States Government. Neither the United States Government nor any agency Thereof, nor any of their employees, makes any warranty, express or implied, or assumes any legal liability or responsibility for the accuracy, completeness, or usefulness of any information, apparatus, product, or process disclosed, or represents that its use would not infringe privately owned rights. Reference herein to any specific commercial product, process, or service by trade name, trademark, manufacturer, or otherwise does not necessarily constitute or imply its endorsement, recommendation, or favoring by the United States Government or any agency thereof. The views and opinions of authors expressed herein do not necessarily state or reflect those of the United States Government or any agency thereof.

DISCLAIMER

Portions of this document may be illegible in electronic image products. Images are produced from the best available original document.

WRITTEN BY: P. J. Legendre	**ATOMICS INTERNATIONAL** *A Division of North American Aviation, Inc.* **TECHNICAL DATA RECORD**	TDR NO. 3552
SECTION: Engineering		GO 7508
GROUP: General Engineering		LEDGER ACCT. 3621
UNIT: Shielding		SUB-ACCT. 4963
APPROVED BY: (SUPERVISOR) R. L. Ashley	PROGRAM: HNPF	TWR 6993
OTHER: S. Berger S. B.	PROJECT: Reactor Structure	DATE March 27, 1959
		PAGE 1 OF 30

TO: L. M. Flower

COPIES TO:

E. B. Ash	H. F. Donohue	M. P. Heisler	E. Matlin
R. L. Ashley	F. L. Fillmore	J. K. Imig	J. Owens
S. Berger	R. C. Gerber	R. E. Johnston	W. E. Parkins
K. E. Buttrey	L. Glasgow	R. H. Karcher	I. E. Randall
D. F. Casey	W. V. Haberer	J. E. Mahlmeister	G. L. Wegmann

SUBJECT: Radial Thermal and Fast Neutron Flux Distributions in the Sodium Reactor Experiment (SRE) and in the Title I Configuration of the Hallam Nuclear Facility (HNPF)

CONTENTS:

I. [illegible]

To determine the thermal neutron flux distribution for the HNPF radial shield in order to establish the heat generation rate distribution in this region.

II. SUMMARY OF RESULTS AND RECOMMENDATIONS

A. SRE Radial Shield

The thermal neutron flux distribution is plotted on Figure 1 for three cases: Case A is the thermal neutron flux distribution normalized to the average thermal neutron flux in the core; Case B is the thermal neutron flux distribution based on meager experimental data(22), and Case C is the thermal neutron flux distribution normalized to the fast neutron flux, as calculated from removal theory, at the core-reflector interface.

The results of the flux calculations (see Figure 1) indicate that the flux distribution of Case A is higher in all regions exterior to the core, whereas that of Case C is lower in all regions except in the concrete. Since it appears to yield the higher fluxes, and hence will result in higher heat generation rates, the method of Case A is preferred in this analysis.

It should be noted that the various SRE experimental results discussed in this report indicate that the Case A thermal neutron flux distribution will be conservative, but the degree of conservatism is not adequately known.

Due to the apparent conservatism in the SRE thermal neutron flux distribution calculations, it is felt that the calculations for the thermal neutron flux distribution in the HNPF Radial Shield will also be conservative, since the radial shield configurations of both reactors are similar.

The fast neutron flux distribution corresponding to the Case A thermal neutron flux distribution is plotted on Figure 2.

B. HNPF Radial Shield

The arrangement of the hexagonal graphite reflector cans in the HNPF forms an irregular outer perimeter, the thickness of which varies between $11\frac{1}{2}$ and $25\frac{1}{2}$ inches of graphite. In order to determine the magnitude of possible hot spots in the side shielding, it was necessary to calculate the fast and thermal neutron flux distributions for three cases of reflector thicknesses. The resulting thermal and fast neutron flux distributions are plotted on Figures 3 and 4, respectively, for the three cases of reflector thickness.

The resulting thermal neutron flux distribution for the SRE and HNPF shield regions, based on the Case A normalization, should be used for the radial shield heat generation rate calculations.

Since the method of calculation is the same for the SRE and HNPF, and the shield configurations of both reactors are similar, the conservatism in the HNPF results will probably be comparable to that for the SRE.

III. METHOD USED

A. Introduction

Information concerning the thermal neutron flux distribution in the radial shield of the HNPF reactor was required in a relatively short time in order to calculate the heat generation rates in this region for the Title I configuration. After conferring with the personnel in the Shielding Unit, it was decided that the method used by R. H. Karcher [(1)] to determine the thermal neutron flux distribution in the bottom shield of the HNPF reactor would be applicable to this problem. This method, without modification, was used to determine the relative neutron fluxes in the radial reflector and shield regions.

In order to determine the adequacy of the HNPF calculations for the thermal neutron flux and heat generation rate distributions, the same calculational methods were applied to the SRE, and these results were compared to experimental data. The result of this comparison indicated that the SRE calculations were somewhat conservative, hence the HNPF calculations should also be conservative to about the same degree.

Table I lists the compositions and temperatures for the core, reflector, and shield regions in the radial directionsof the SRE. The temperatures in the regions between the outer half of the core and the outside of the thermal shield were found experimentally (3) to vary between 712° F and 692° F during an 88-hour test run at an indicated reactor power level of 20.4 MWt. Therefore, in the neutron calculations, the temperatures of the regions between the reflector and the insulation were assumed to be 700° F. Subsequent experiments (14) showed the concrete temperature to be about 120° F; hence, the temperatures of the insulation, cavity liner, and concrete were assumed to be 300° F, 150° F, and 150° F, respectively.

Table II lists the compositions and temperatures for the core, reflector, and shield regions in the radial direction of the HNPF. The non-referenced temperatures in Table II were assumed on the basis of the referenced temperatures.

Since the arrangement of the hexagonal graphite reflector cans forms an irregular outer perimeter, the neutron flux distribution in the HNPF radial shield was calculated for the minimum, average, and maximum reflector thicknesses which would exist. These calculations were performed in order to determine the magnitude of possible hot spots in the side shielding. The reflector and the adjacent sodium region thicknesses used in these calculations are listed in Table II.

Table III lists the fast neutron removal cross sections for the SRE and HNPF. The four group constants used in the radial neutron flux calculations for the SRE and HNPF are listed in Tables IV and V, respectively.

In calculating the heat generation rates in the radial shields of the SRE and HNPF, the "GRACE I" (24) gamma-ray heat generation code was used. The source strengths for each source region were obtained using the thermal neutron flux distributions presented in this report. The GRACE I code was written for a slab geometry, which closely approximates the closely spaced concentric cylindrical geometry of the SRE and HNPF systems. Therefore, the slab geometry approximation was used in all the neutron flux calculations in this report, the resulting thermal neutron flux distributions being slightly conservative. At the core-reflector interface, the slab geometry results were approximately 19% (25) more conservative than those calculated using cylindrical core geometry, while on the outside of the thermal shield, they were about 4½% (25) more conservative.

B. Core Constants

1. Origin

The four-group core constants for the HNPF (listed in Table IV A) were obtained from the Experimental Neutron Physics Group [16], whereas the four-group core constants for the SRE (listed in Table VIII) were calculated using the same techniques as for the HNPF core constants. This method utilized the Westinghouse Fast Neutron Spectrum Code "MUFT-4" [17]. The diffusion coefficients (D, cm) for all four energy groups of the HNPF and for the fourth energy group (thermal) of the SRE were calculated using four-group constants obtained from L. A. Wilson [15].

2. Self-shielding number for the SRE MUFT-4 input.

The self-shielding number, L_{MUFT}, applies to the elements with resonances [17]; U^{238} is the only resonance case considered in this problem. L_{MUFT} is defined as

$$L_{MUFT} = \alpha \chi \sqrt{\frac{S_f}{M_{238}}}$$

where M_{238} = mass of U^{238}, 364 gm/cm of height [4]

S_f = surface area of a fuel cell, 19.31972 cm^2/cm of height [19]

The Doppler broadening factor, χ, is given by the following relationship:

$$\chi = 1.5 \times 10^{-5} (t_f - 300^\circ K) + 1 = 1.007$$

where t_f = fuel temperature, $773^\circ K$ [4]

The resonance shadowing factor, α, is a function of λ_s / L [20] where λ_s, the scattering mean free path $(=1/\Sigma_s)$ is determined as follows [4,15]:

$$\Sigma_{tr} = 0.9445\, \Sigma_s + \Sigma_{a4}$$

where Σ_{tr} = macroscopic transport cross section, 0.3723 cm^{-1} [4]

Σ_{a4} = macroscopic absorption cross section, 0.0023 cm^{-1} [4]

The factor L represents the following collection of terms:

$$L = \frac{4\, V_m}{S_f} \qquad (4)$$

where V_m = volume of the moderator, cm^3/cm of height, and this is, in turn calculated from

$$V_m = V_f A_h \qquad (5)$$

where V_f = volume fraction of the moderator, 0.855798[4]

A_h = cross section area of a cell, cm^2

$$A_h = \sqrt{\frac{3}{2}}\, \ell^2 \qquad (6)$$

where ℓ = distance across the flats of a cell, 10.910 in.[4]

For $\eta\, s/L$ = 0.0226, and α = 0.988[20], Equation (1) gives L_{MUFT} = 0.217 cm-gm$^{-\frac{1}{2}}$.

3. Summary

The SRE MUFT-4 input data is listed in Table VII, and the four-group SRE core constants are listed in Table VIII.

C. Thermal Neutron Flux Distribution Obtained by Experiment [22]

Experimental measurements of thermal neutron flux were obtained about July, 1957, at a power level of nearly 2 kwt with a 34 element loading. In extrapolating the experimental results to 20 MWt, several items were considered. It was established [31] that the thermal power level instrument indicating the 2 kw of power had an uncertainty of about 20 per cent based upon the power instrument calibration. In the report [22] published October 15, 1958, the power level for the experiment was given as 1.9 kwt. Therefore, to permit proper extrapolation to 20 MWt power, an extrapolation factor will be required. The calculation of this factor considers that the power level indicator reading was 20% high at a power level of 2 kwt. The factor, F, was calculated in the following manner.

$$F = \frac{\phi_{20}}{\phi_{.002}} = \frac{P_{20}/V_{20}\Sigma_f}{P_{.002}/V_{.002}\Sigma_f} \qquad (7)$$

where ϕ_{20} = thermal neutron flux at 20 MWt, n/cm^2-sec.

$\phi_{.002}$ = thermal neutron flux at .002 MWt, n/cm^2-sec.

V_{20} = core volume at 20 MWt (a 43 fuel element loading is assumed)

$V_{.002}$ = core volume at .002 MWt (a 34 fuel element loading is assumed)

P_{20} = 20 MWt

$P_{.002}$ = (.8)(.002) = .0016 MWt

$$F = \frac{20/43}{.0016/34} = 0.99 \times 10^4$$

$$F \approx 10^4 \pm 20\%$$

It was noted that Figure 5 of reference 22 did not show a sodium region between the reflector and the stainless steel core liner. Since this sodium region is very important in the gamma-ray heat generation calculations (which are based upon the thermal neutron flux distributions described in this report), it was necessary to alter the fluxes presented in Figure 5 to account for the existence of several additional regions between the reflector and thermal shield. These fluxes were altered as follows:

$$\phi_1 = \phi_0 \; e^{-\mathcal{H} x}$$

where ϕ_0 = thermal neutron flux entering the region, n/cm^2-sec.

ϕ_1 = thermal neutron flux leaving the region, n/cm^2-sec.

x = region thickness, cm.

$\mathcal{H}$ = thermal neutron attenuation coefficient in the region, cm^{-1}

The values of $\mathcal{H}$ were estimated on the basis of previous calculations (22,34); the values for $\mathcal{H}$ are tabulated below

Region	$\mathcal{H}$, cm^{-1}
Inner Sodium	0.0350
Core Liner	.640
Outer Sodium	.0350
Core Tank	.229 (22)

The resulting thermal neutron flux distribution is plotted on Figure 1 of this report.

D. Normalization of the Relative Neutron Flux Distribution Obtained from the WANDA Code for the SRE.

1. Introduction

As mentioned previously, in order to determine the adequacy of the calculational techniques being used in the HNPF radial heat generation analysis, it was decided to perform similar calculations for the SRE and compare the results with experiment. Since the major source of heating in the radial shielding was anticipated as being due to capture gamma rays created in the thermal shield regions, the comparison could be made on the basis of calculated and measured thermal neutron flux distributions. Two methods of calculating the SRE neutron flux distributions were proposed; in both cases results obtained from the WANDA code were to be used. These results were normalized by two different procedures. In the first method, the thermal neutron flux from the WANDA code was normalized to the average thermal neutron flux in the core, whereas, in the second method, the fast neutron flux from the WANDA code was normalized to the fast neutron flux at the core-reflector interface, as calculated by removal theory. The details of these two methods are discussed below.

2. Normalization to the average thermal neutron flux in the core

The average thermal neutron flux in the core, $\bar{\phi}_{th}$ in n/cm^2-sec is determined from the following expression:

$$\bar{\phi}_{th} = \frac{P\,F}{V\,\Sigma_f} \qquad (9)$$

where P = rated power of the core, 20 Mwt (6.2×10^{17} fis/sec)
V = volume of the core, 5.33×10^6 cm^3

where Σ_f = macroscopic fission cross section of the core, 0.00342 cm^{-1}

F = the ratio of the number of fissions produced by thermal neutrons to the number of fissions produced by neutrons of all energies.

In a report by A. R. Vernon [26], the ratio, F, of the number of fissions due to the thermal neutrons to the number of fissions due to neutrons at all energies was about 0.50 at the core-reflector interface. The specific activity of the reactor sodium; based on the thermal neutron flux presented in the referenced report [26], was 0.27 curies per gm. However, the results of earlier work by A. R. Vernon [35] indicated a sodium specific activity of 0.37 curies per gm. By assuming that the specific activity is directly proportional to the ratio F, 0.37 curies per gm corresponds to F=0.685. On the other hand, recent experimental results [27] yielded a Na^{24} specific activity of 0.19 curies per gm at a reactor power level of 13.5 MWt. The power level was measured with gold foils, and the estimated experimental uncertainty was about 20%. A linear extrapolation of the Na^{24} specific activity to 20 MWt resulted in a value of 0.30 curies per gm [27]. By assuming this latter value of the sodium activity to be proportional to F, a value of F = 0.555 is obtained. It can be seen from the above that the value of F lies somewhere between 0.50 and 0.70, and therefore, for the purposes of this calculation it is assumed that F = 0.70, the uncertainty being about 20%.

Substituting in Equation (9) with F = 0.70 yields $\bar{\phi}_{th} = 2.38 \times 10^{13}$ n/cm^2-sec.

The peak thermal neutron flux at the center of the core, ϕ_o is determined in the following expression:

$$\phi_o = \bar{\phi}_{th} \left[\frac{\phi_o}{\bar{\phi}_{th}}\right]_R \left[\frac{\phi_o}{\bar{\phi}_{th}}\right]_A \qquad (10)$$

where $\left[\frac{\phi_o}{\bar{\phi}_{th}}\right]_R$ = ratio of radial peak-to-average thermal neutron flux, and this, in turn, is determined from the following:

$$\left[\frac{\phi_o}{\bar{\phi}_{th}}\right]_R = \frac{\phi_o}{\frac{\int \phi \, dV}{V}} \qquad (11)$$

where ϕ_o = relative peak thermal neutron flux in the core, 0.3743 n/cm^2-sec

$\int \phi dV$ = integrated thermal neutron flux in the core, 29.23 n-cm/sec.

V = integrated volume of the core, 95.6 cm^3

The values of ϕ_o, $\int \phi dV$ and V were obtained from the same WANDA output data that gave the values of the relative neutron fluxes.

From these values, $\left.\dfrac{\phi_o}{\bar{\phi}_{th}}\right]_R = 1.22.$

The ratio of the axial peak-to-average thermal neutron flux,

$\left.\dfrac{\phi_o}{\bar{\phi}_{th}}\right]_A$, was calculated previously[4], and was taken, without change,

to be $\left.\dfrac{\phi_o}{\bar{\phi}_{th}}\right]_A = 1.236$

Substituting in Equation (10) gives

$$\phi_o = 3.60 \times 10^{13} \text{ n/cm}^2\text{-sec}$$

The preceding absolute peak thermal neutron flux in the core region was set equal to the relative peak thermal neutron flux in the core region, the latter having been obtained from the WANDA II calculations. This normalizes the relative neutron flux distribution to the absolute neutron flux distribution. The resulting absolute thermal and fast neutron flux distributions are plotted on Figures 1 and 2, respectively.

3. Normalization to the fast neutron flux, calculated from fast neutron removal theory, at the core-reflector interface.

The fast (Group 1) neutron flux ϕ_1 in neutrons/cm^2-sec, at the core reflector interface of a slab reactor is determined from the following equation:

$$\phi_1 = \frac{S_V}{2\Sigma_R}$$

where Σ_R = fast removal cross section of the core, 0.02027 cm^{-1}

The group one neutron volumetric core source strength, S_V, in n/cm^3-sec, is calculated as follows:

$$S_V = \frac{C\,P}{V}\nu$$

where ν = 2.47 fast neutrons per fission
C = 3.1×10^{10} fissions per watt-sec
P = reactor power, 2×10^7 watts
V = core volume, 5.33×10^6 cm^3

Substitution in Equation (12) gives $\phi_1 = 7.10 \times 10^{12}$ n/cm^2-sec

The preceding absolute fast neutron flux at the core-reflector interface was set equal to the relative fast neutron flux at the same position, the latter having been obtained from the WANDA II calculations. This normalizes the relative neutron flux distribution to the absolute neutron flux distribution. The resulting absolute thermal neutron flux distribution is plotted on Figure 1.

E. Normalization of the Relative Neutron Flux Distribution Obtained from the WANDA Code for the HNPF

Comparison of the flux distributions in the SRE, as calculated in Sections III D.2 and 3, indicates that the results obtained using the method of Case A are preferable since, from comparison with experiment, Case A fluxes are higher and, hence, will yield more conservative data. This method was therefore chosen to evaluate the flux distributions in HNPF.

The specific values of the constants used for HNPF are listed below:

P = 254 MWt
V = 5.44×10^7 cm^3
F = 0.731 (28)
Σ_f = 0.00388 cm^{-1} (16)

Substituting these values into Equation (9) yields $\bar{\phi}_{th} = 2.72 \times 10^{13}$ n/cm^2-sec.

To obtain the peak value in the core, Equation (10) is used with

$$\left.\frac{\phi_o}{\phi_{th}}\right]_R = 1.76^{(29)}$$

$$\left.\frac{\phi_o}{\phi_{th}}\right]_A = 1.40^{(29)}$$

Substitution yields ϕ_o 6.7×10^{13} n/cm²-sec.

The absolute peak thermal neutron flux in the core, ϕ, is set equal to the relative peak thermal neutron flux in the core, and the relative neutron flux distribution in the reactor adjusted accordingly.

The thermal and fast neutron flux distributions in the HNPF are plotted on Figures 3 and 4, respectively, for the three cases of reflector thickness.

F. Discussion

In order to establish both a consistent calculational procedure for obtaining the neutron flux distribution in the HNPF radial shield, and to determine its accuracy; it was decided to apply several different calculational methods to obtain the thermal neutron flux distribution in the SRE and compare the results with experiment.

With regard to the experimental measurements, several sets of data were available. The most complete set of data has been published by Fillmore and Doyas(22), who report a radial thermal neutron flux distribution through the core and reflector and into the concrete. However, in the plotting of their experimental data, a sodium region, located between the reflector and the core liner, was omitted. The data reported in the reference(22) was altered to account for this; the resultant flux distribution being shown in Figure I.

Several other experimental measurements have been reported in various instrument thimbles. For example, an experiment(30) was performed to determine the gamma-ray dose rate in the instrument thimbles as well as the simultaneous neutron and gamma-ray dose rate decay after shutdown in the SRE. The thermal neutron flux in the #8 instrument thimble measured 2.2×10^9 n/cm²-sec at a power level of 20.2 MWt, which extrapolates to 2.17×10^9 n/cm²-sec at 20 MWt. However, the #8 instrument thimble faces a 2-3/4 in. x 12 in. diameter hole which is cut into the thermal shield rings so that a valid correlation with the calculated thermal neutron flux in this report cannot be made. At the point next to the vessel wall, instrument thimble #8 is located, this report gives 1.7×10^9 n/cm²-sec for no cutout. If 2-3/4 in. of the thermal shield is removed, from the data shown in Figure 1, a rough value of about 2×10^{10} n/cm^2-sec is obtained.

From SRE experiments [31,32] performed prior to the preceding experiment, data from instrument thimble #5 yielded a thermal neutron flux of 1.1×10^9 n/cm^2-sec at a power level of 18.5 MWt. However, this value was given with reservation [32] due to the somewhat crude calibration of the instruments [32] and the extrapolations of data [31,32] involved. This thermal neutron flux extrapolates to 1.19×10^9 n/cm^2-sec at a power level of 20 MWt, while 1.7×10^9 n/cm^2-sec is the comparable value given in this report, and Fillmore and Doyas report 1.5×10^9 n/cm^2-sec[22].

However, there are indications [32,33] of an indirect correlation between the calculated and experimental thermal neutron flux values. The measured gamma-ray dose rate in the #7 instrument tube, which does not have a cutout in the thermal shield, and extrapolated to 20 MWt was 62,600 r/hr [33]. The calculated gamma-ray dose rate using the thermal neutron flux distribution from this report was 51,000 r/hr [33].

In view of the experimental results obtained from the SRE, as discussed earlier in this section, there are indications that the thermal neutron flux distribution as calculated in this report for the SRE may be conservative, but the degree of conservatism is not adequately known.

Due to the apparent conservatism in the SRE thermal neutron flux distribution calculations (as determined by the method presented in this report), it is felt that the calculations for the thermal neutron flux distribution in the HNPF will also be conservative, since the calculational method used for the HNPF is the same as that for the SRE.

IV. REFERENCES AND APPENDICES

1. R. H. Karcher, "Evaluation of Nuclear Heat Generation in the Hallam Nuclear Facility Bottom Shield Reactor Support Structure as Proposed in Title I," TDR-2931, August 6, 1958.

2. F. L. Fillmore, "Multigroup Theory for Non-Multiplying Regions and Application to the SRE Shield Calculations," NAA-SR-Memo-1069, August 13, 1954.

3. W. Littleton, "Reactor High Temperature Data," IOL to S. V. McKeever, September 2, 1958.

4. F. L. Fillmore, "Two-Group Calculation of the Critical Core Size of the SRE Reactor," NAA-SR-1517, July 1, 1956.

5. "Installation-Core Tank," AI Drawing No. 9693-792131, November 5, 1955.

6. J. E. Mahlmeister, "HNPF Design Data - Reactor Core," Systems Description, June 24, 1958.

7. Personal Communication, J. S. Stewart, General Engineering Group, Atomics International.

8. G. W. Grodstein, "X-ray Attenuation Coefficients from 10 kev to 100 Mev," U. S. National Bureau of Standards Circular 583, Washington, D.C., U.S. Government Printing Office, April 30, 1957.

9. Personal Communication, R. H. Karcher, General Engineering Group, Atomics International.

10. "Reactor General Arrangement, Hallam Nuclear Power Facility," AI Drawing No. 7508-71001, July 7, 1958. Information Print, July 7, 1958.

11. F. D. Anderson, "Analysis of the Equilibrium Specific Activity of the Primary Sodium in the Hallam Nuclear Power Facility (HNPF) and the Sodium Reactor Experiment (SRE)," TDR-2592, August 8, 1958.

12. Personal Communication, T. Ricci, Design Group, Atomics International.

13. G. T. Chapman, G. L. Storrs, "Effective Neutron Removal Cross Sections for Shielding," AECD-3978, September 19, 1955.

14. W. Littleton, "Concrete Temperatures at SRE Full Power Operation," IOL to D. F. Casey, S. V. McKeever, and R. L. Tomlinson, October 9, 1958.

15. Personal Communication, L. A. Wilson, Compact Power Reactor Group, Atomics International.

16. Personal Communication, R. J. Doyas, Experimental Neutron Physics Group, Atomics International.

17. H. Bohl, Jr., E. M. Gelbard, and G. H. Ryan, "MUFT-4, Fast Neutron Spectrum Code for the IBM-704," WAPD-TM-72, July, 1957.

18. Delete.

19. R. O. Williams, "SRE Criticality Calculations," NAA-SR-Memo-1082, October 25, 1954.

20. W. D. Leggett, "Nuclear Calculations for AKS OMR Proposal," TDR-3036, September 18, 1958.

21. R. L. Ashley, "Preliminary Draft of a Shielding Data Manual," NAA-SR-Memo 1187, Revised, December 9, 1954.

22. F. L. Fillmore and R. J. Doyas, "Analysis of Neutron Flux in the Shielding of the Sodium Reactor Experiment," NAA-SR-2953, October 15, 1958.

23. Delete.

24. D. S. Duncan, "GRACE I Gamma-Ray Attenuation Code in Slab Geometry," NAA Program Description, Deck No. W3-142, December, 1957.

25. R. E. Johnston, TDR to be published.

26. A. R. Vernon, "Analysis of the Biological Shield of the Sodium Reactor Experiment," NAA-SR-1949, June 15, 1957.

27. R. L. Tomlinson, "HNPF Shielding Hilites for the Week Ending December 4, 1958," IOL to J. E. Mahlmeister and H. A. Ross-Clunis, December 4, 1958.

28. Personal Communication, K. E. Buttrey, General Engineering Group, Atomics International.

29. R. C. Gerber, "HNPF Review with Reactor Hazards Evaluation Board," IOL to R. L. Olson, October 27, 1958.

30. H. F. Donohue, "Neutron and Gamma Flux Survey of the SRE Instrument Thimbles," TDR 3131, October 8, 1958.

31. R. L. Tomlinson, "Experimental Evaluation of the Neutron Streaming in the SRE Galleries as Measured During the First Two Power Runs of the SRE," TDR 2202, October 17, 1957.

32. R. L. Tomlinson and E. B. Ash, "Measurement of the Neutron Flux and Gamma-Ray Dose Rate During Full Power SRE Operation and Subsequent to Scheduled 'Δ t' 'Scram'," TDR 2933, August 8, 1958.

33. R. E. Johnston, "Comparison of Calculated Gamma-Ray Dose Rates at SRE Instrument Thimbles to the Measured Gamma-Ray Dose Rates," TDR to be published.

34. J. S. Stewart, "Analysis of the Heat Generation in the Side Shield for the HNPF Reactor-Reference Configuration," TDR-2996, August 17, 1958

35. A. R. Vernon, "Activity of Primary Sodium in SRE," IOL to W. E. Parkins, April 27, 1955.

TABLE I

A: SRE Shield Region Composition (gm/cc)

Region*	Core[4]	Reflector[4]	Sodium	Core[7] Liner	Sodium	Core[7] Tank	Thermal Shield	Vessel Wall	Insulation[9]	Cavity Liner	Ordinary[8] Concrete
Temp. °F		877[2]	700	700	700	700	700	700	300	150	150
Radial Thickness (in.)	37.7	22.5	1.50[5]	.25[5]	2.5[5]	1.50[5]	5.50[5]	.25[5]	9.0[5]	.25[5]	36
$Uranium^{235}$	.01485										
$Uranium^{238}$	.524										
Potassium	.000248										.0450
Zirconium	.111	.0806									
Sodium	.0572	.0240	.835		.835						.0400
Graphite	1.395	1.57									
Iron	.0153			5.20		5.20	7.85	7.85	.0153	5.20	.0286
Silicon	.000458			.115		.115			.135	.115	.734
Magnesium									.0162		.00562
Aluminum									.0108		.106
Oxygen									.181		1.16
Nickel	.00206			.698		.698				.698	
Manganese	.000458			.155		.155				.155	
Chromium	.00435			1.47		1.47				1.47	

TABLE I-A (Continued)

Region*	Core (4)	Reflector (4)	Sodium	Core Liner (7)	Sodium	Core Tank (7)	Thermal Shield	Vessel Wall	Insulation (9)	Cavity Liner	Ordinery Concrete (8)
Phosphorus	.000229			.0774		.0774				.0774	
Hydrogen											.0131
Sulfur											.00281
Calcium											.193

B: SRE Core Temperature Breakdown (4)

Component	Temperature, (°F)
Fuel	932
Stainless Steel	770
NaK	788
Zirconium	752
Sodium	734
Graphite	797

* The reference noted by each region's name indicates the original source of information from which the component densities (gm/cc) were computed.

730-Q-8

TABLE II

A: HNPF Shield Region Composition (gm/cc)

Region*	Core[6]	Reflector[6]	Sodium	Vessel Liner	Sodium	Core Tank	Containment Tank	Thermal Shield 1	Thermal Shield 2	Insulation[9]	Cavity Liner	Ordinary Concrete[8]
Temp. °F	945[6]	776	776[11]	776	776[11]	776	776	1000	1000	600	200	200
Radial Thickness (in.)	81	See Table II B	See Table II B	.5[12]	3.5[10]	.75[10]	.25[10]	2.75[10]	2.75[10]	.12[10]	.5[10]	60[10]
Uranium 235	.0170											
Uranium 238	.463											
Oxygen	.0673									.181		1.16
Stainless Steel	.058	.0441		7.85		7.85	7.85					
Graphite	1.33	1.46										
Sodium	.0736	.0292	.82		.82							.0400
Zircaloy II	.00451											
Iron								7.85	7.85	.0153	7.85	.0286
Silicon										.135		.734
Magnesium										.0162		.00562
Aluminum										.0108		.106
Potassium												.0450
Hydrogen												.0131
Sulfur												.00281
Calcium												.191

* The reference noted by each region's name indicates the original source of

TABLE II (Continued)

B: Reflector and the Adjacent Sodium Region Thickness (in.)[10]

	Reflector	Sodium
Maximum	25.5	4.5
Average	19	11
Minimum	11.5	18.5

TABLE III

Fast Neutron Removal Cross Sections (13)

A: SRE

Region	Σ_R, cm^{-1}
Core	0.0667
Reflector	.0656
Sodium	.0336
Core Liner	.168
Sodium	.0336
Core Tank	.168
Thermal Shield	.168
Vessel Wall	.168
Insulation	.0102
Cavity Liner	.168
Concrete	.0768

B: HNPF

Region	Σ_R, cm^{-1}
Core	0.0654
Reflector	.0626
Sodium	.0336
Vessel Liner	.168
Sodium	.0336
Core Tank	.168
Containment Tank	.168
Thermal Shield 1	.168
Thermal Shield 2	.168
Insulation	.0102
Cavity Liner	.168
Concrete	.0768

TABLE IV

Four Group Constants(1,15) for the SRE

Region	Σa_1 (cm^{-1})	Σr_1 (cm^{-1})	D_1 (cm)	Σa_2 (cm^{-1})	Σr_2 (cm^{-1})	D_2 (cm)	Σa_3 (cm^{-1})	Σr_3 (cm^{-1})	D_3 (cm)	Σa_4 (cm^{-1})*(21)	D_4 (cm)
Reflector	0.000	0.0176	1.91	0.000016	0.0275	0.985	0.000	0.0291	0.938	0.000255	0.938
Sodium	.000	.00751	4.50	.000	.0171	.975	.000774	.00353	4.80	.00774	4.71
Core Liner	.00453	.0447	1.44	.0105	.0111	.533	.0162	.0158	.371	.150	.406
Sodium	.000	.00681	4.50	.000	.0171	.975	.000774	.00353	4.80	.00774	4.71
Core Tank	.00453	.0433	1.44	.0105	.0111	.533	.0162	.0158	.371	.150	.406
Thermal Shield	.00275	.0580	1.60	.0114	.0090	.644	.0129	.0162	.361	.129	.361
Vessel Wall	.00275	.0472	1.60	.0114	.0090	.644	.0129	.0162	.361	.129	.361
Insulation	.000265	.000835	11.5	.000197	.00187	9.88	.00005	.00179	10.3	.00062	9.35
Cavity Liner	.00453	.0388	1.44	.0105	.0111	.533	.0162	.0158	.371	.208	.406
Concrete	.00146	.0105	1.73	.00104	.0372	1.26	.000473	.0437	1.33	.00636	1.065

*Values of Σa_4 are temperature corrected to the temperatures listed in Table I.

TABLE V
Four Group Constants (1,15) for the HNPF

Region	Σ_{a_1} (cm^{-1})	Minimum Reflector Σ'_{r1} (cm^{-1})	Average Reflector Σ'_{r1} (cm^{-1})	Maximum Reflector Σ'_{r1} (cm^{-1})	D_1 (cm)	Σ_{a_2} (cm^{-1})	Σ_{r_2} (cm^{-1})	D_2 (cm)
Reflector	0.0000286	0.0222	0.0184	0.0165	2.02	0.000062	0.0263	1.01
Sodium	.0000825	.00795	.00664	.00612	4.50	.0000678	.0171	.975
Vessel Liner	.00453	.0535	.0615	.0610	1.44	.0105	.0111	.533
Sodium	.0000825	.00795	.00550	.00648	4.50	.0000678	.0171	.975
Core Tank	.00453	.0523	.0639	.0442	1.44	.0105	.0111	.533
Containment Tank	.00453	.0645	.0603	.0670	1.44	.0105	.0111	.533
Thermal Shield 1	.00275	.0574	.0535	.0558	0.60	.0114	.0090	.644
Thermal Shield 2	.00275	.0513	.0535	.0623	1.60	.0114	.0090	.644
Insulation	.000265	.00177	.00132	.000468	11.5	.000197	.00187	9.88
Cavity Liner	.00275	.0373	.0520	.0585	1.60	.0114	.0090	.644
Concrete	.00146	.0102	.0100	.0102	1.73	.00104	.0372	1.26

TABLE V (Continued)

Region	Σ_{a_3} (cm^{-1})	Σ_{r_3} (cm^{-1})	D_3 (cm)	Σ_{a_4} (cm^{-1}) *(21)	Σ_{r_4} (cm^{-1})	D_4 (cm)
Reflector	0.000138	0.0274	0.988	0.00127	0.000	0.988
Sodium	.000774	.00353	4.80	.00746	.000	4.71
Vessel Liner	.0162	.0158	.371	.145	.000	.406
Sodium	.000774	.00353	4.80	.00746	.000	4.71
Core Tank	.0162	.0158	.371	.145	.000	.406
Containment Tank	.0162	.0158	.371	.145	.000	.406
Thermal Shield 1	.0129	.0162	.361	.115	.000	.361
Thermal Shield 2	.0129	.0162	.361	.115	.000	.361
Insulation	.0000511	.00179	10.3	.00053	.000	9.35
Cavity Liner	.0129	.0162	.361	.170	.000	.361
Concrete	.000473	.0437	1.33	.00614	.000	1.065

* Values of Σ_{a_4} are temperature corrected to the temperatures listed in Table II.

TABLE VI

A: HNPF Four Group Core Constants (16)

Σ_{r_1} = 0.02086 cm^{-1}

Σ_{a_1} = .000606 cm^{-1}

Σ_{f_1} = .00114 cm^{-1}

Σ_{r_2} = .011 cm^{-1}

Σ_{a_2} = .000619 cm^{-1}

Σ_{f_2} = .000160 cm^{-1}

Σ_{r_3} = .0158 cm^{-1}

Σ_{a_3} = .00265 cm^{-1}

Σ_{f_3} = .00177 cm^{-1}

Σ_{f_4} = .00958 cm^{-1}

B: HNPF Four Group Core Constants (1,15)

D_1 = 1.93 cm

D_2 = .96 cm

D_3 = .837 cm

D_4 = 1.00 cm

C: HNPF Four Group Constants (21)

Σ_{a_4} = .0221 cm^{-1}*

* The values of Σ_{a_4} are temperature corrected to the temperatures listed in Table II

TABLE VII

MUFT-4 Input Data for the Four Group SRE Core Constants

A: Material Densities

Material	*Atomic Density (N_i), barns^{-1}
Zirconium	0.000733
Graphite	.0702
Iron	.000248
Uranium-238	.00133
Sodium	.00133
Uranium-235	.0000381

* Based on the densities listed in Table I

B: Buckling and Self-Shielding Number

$$B^2 = 0.505 \times 10^{-3} \text{ cm}^{-2} \quad (4,19)$$

$$L_{MUFT} = 0.217 \text{ cm}$$

TABLE VIII

Four Group SRE Core Constants

A: MUFT-4 Results

Group	D(cm)	$\Sigma_a(cm^{-1})$	$\Sigma_r(cm^{-1})$	$\nu\Sigma_f(cm^{-1})$
1	2.434	0.000680	0.02027	0.00160
2	1.097	.000544	.000974	.000209
3	.9618	.002505	.00434	.002286

B: Group Four Constants

$D_4 = 0.9148 \ cm^{-1}$ (1,15)

$\Sigma_{a_4} = 0.0198 \ cm^{-1}$

$\nu\Sigma_{f_4} = 0.00845 \ cm^{-1}$

Radial Thermal Neutron Flux Distribution in the SRE

Figure 1 March 27, 1959

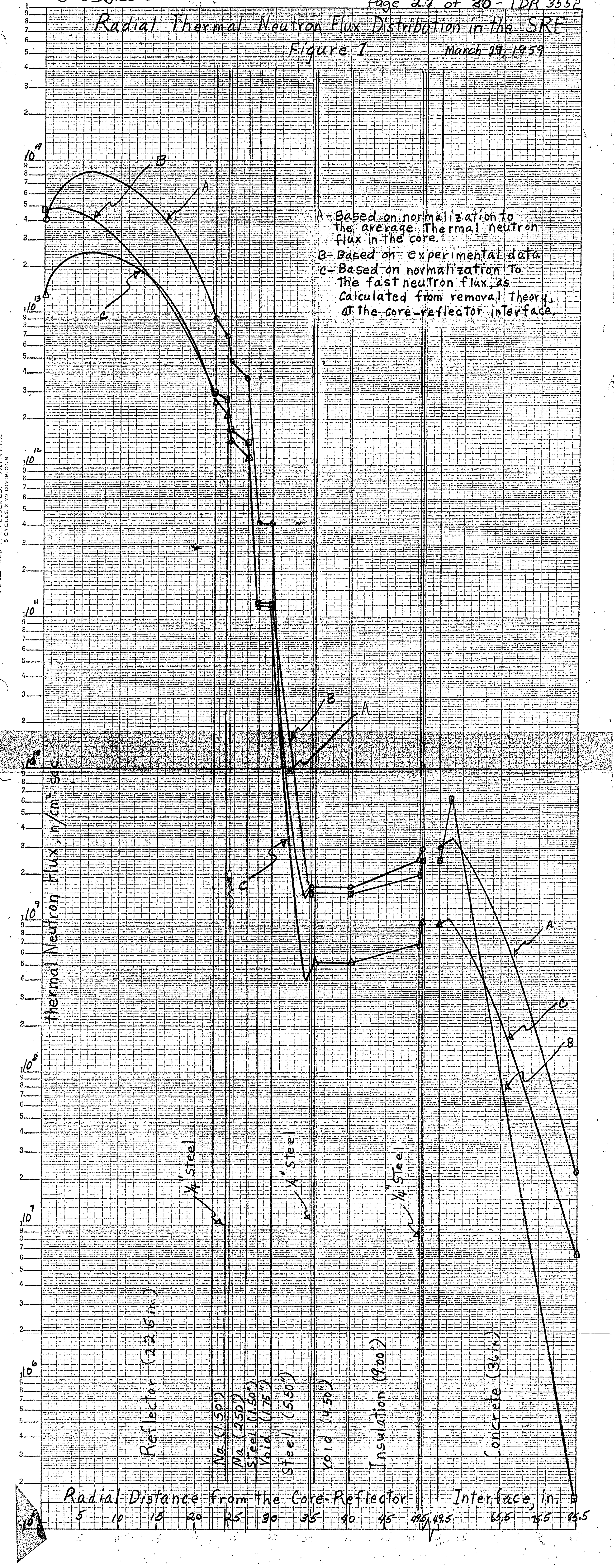

Radial Fast Neutron Flux Distribution in the SRE

Figure 2

27 March 1959

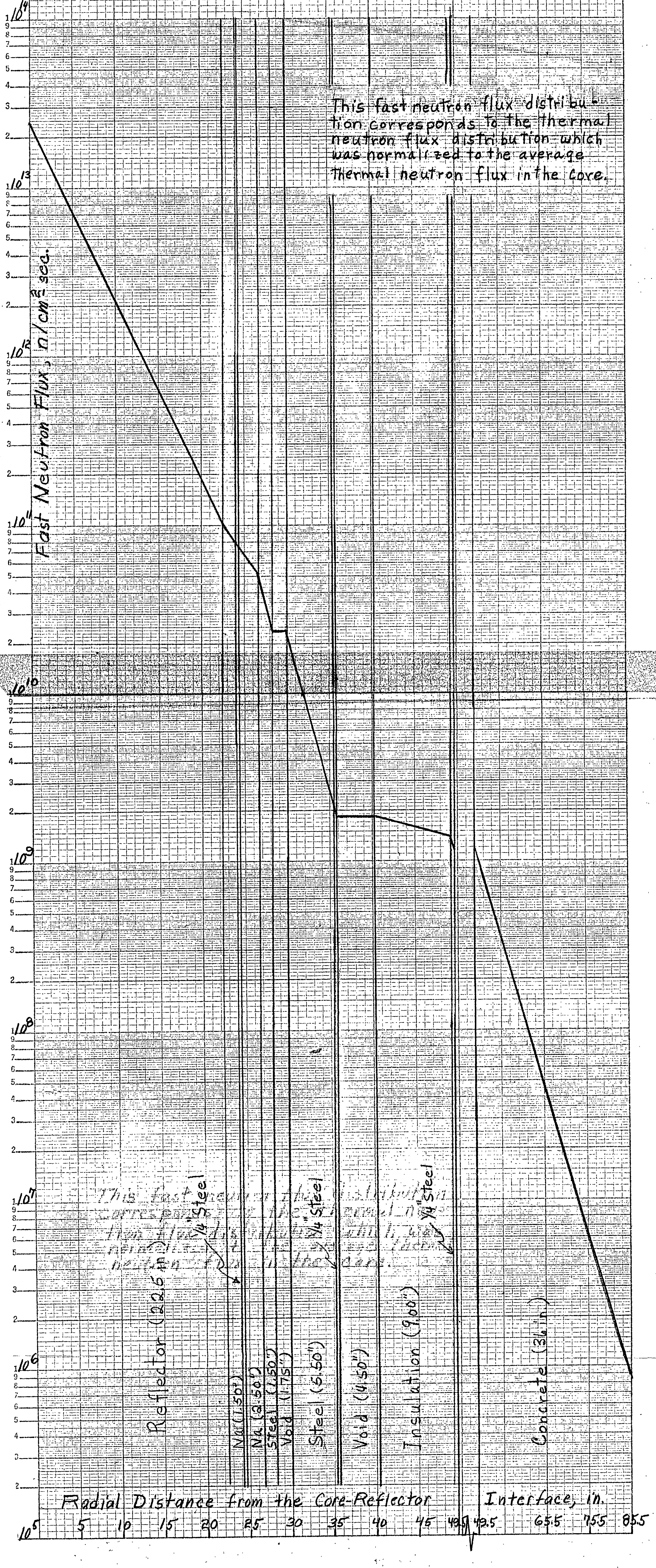

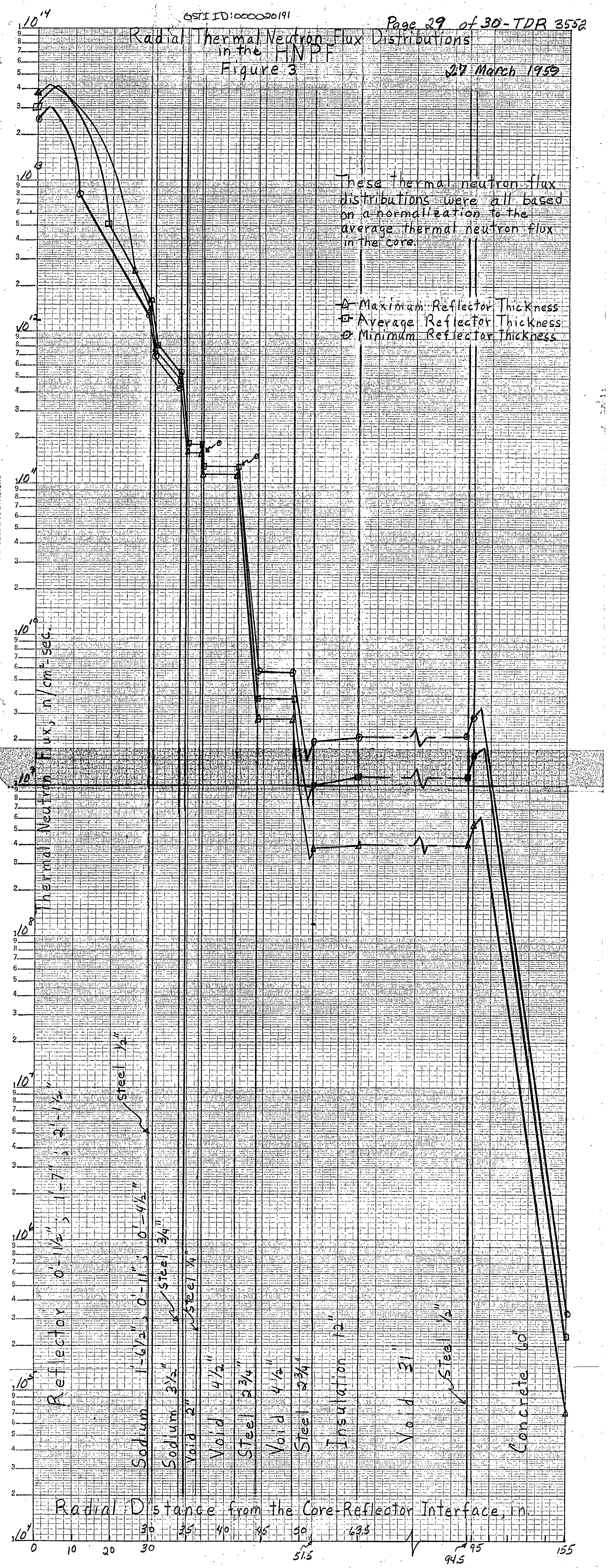
Radial Thermal Neutron Flux Distributions
in the HNPF
Figure 3
27 March 1959
These thermal neutron flux distributions were all based on a normalization to the average thermal neutron flux in the core.
Maximum Reflector Thickness
Average Reflector Thickness
Minimum Reflector Thickness
Thermal Neutron Flux, n/cm²-sec.
Reflector 0'-1½", 1'-7", 2'-1½"
Sodium 1'-6½", 0'-11", 0'-4½"
Steel ½"
Sodium 3½"
Steel ¾"
Void 2"
Steel ¼"
Void 4½"
Steel 2¾"
Void 4½"
Steel 2¾"
Insulation 12"
Void 31"
Steel ½"
Concrete 60"
Radial Distance from the Core-Reflector Interface, in.
SEMI-LOGARITHMIC 359-91
KEUFFEL & ESSER CO.
5 CYCLES X 70 DIVISIONS

Radial Fast Neutron Flux Distributions
in the HNPF
Figure 4

27 March 1959

These fast neutron flux distributions correspond to the thermal neutron flux distributions which were normalized to the average thermal neutron flux in the core.